

Rapid Colorimetric Quantitative Portable Platform for Detection of *Brucella melitensis* Based on a Fluorescence Resonance Energy Transfer Assay and Nanomagnetic Particles

Sahar Alhogail, Raja Chinnappan, Ghadeer A.R.Y. Suaifan, Khalid M. Abu-Salah, Khaled Al-Kattan, Dana Cialla-May, Popp Jürgen, and Mohammed M. Zourob*



Cite This: *ACS Omega* 2024, 9, 20997–21005



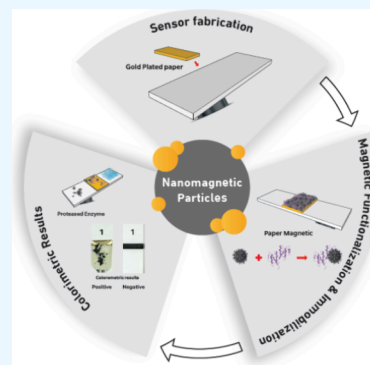
Read Online

ACCESS |

Metrics & More

Article Recommendations

ABSTRACT: Brucellosis is a bacterial zoonotic disease that requires major attention for both health and financial facilities in many parts of the world including the Mediterranean and the Middle East. The existing gold standard diagnosis relies on the culturing technique, which is costly and time-consuming with a duration of up to 45 days. The *Brucella* protease biosensor represents a new detection approach that will lead to low-cost point-of-care devices for sensitive *Brucella* detection. In addition, the described diagnostic device is portable and simple to operate by a nurse or non-skilled clinician making it appropriate for the low-resource setting. In this study, we rely on the total extracellular protease proteolytic activity on specific peptide sequences identified using the FRET assay by high-throughput screening from the library of peptide (96 short peptides such as dipeptides and tripeptides) substrates for *Brucella melitensis* (*B. melitensis*). The *B. melitensis*-specific protease substrate was utilized in the development of the paper-based colorimetric assay. Two specific and highly active dipeptide substrates were identified (FITC-Ahx-K-r-K-Ahx-DABCYL and FITC-Ahx-R-r-K-Ahx-DABCYL). The peptide-magnetic bead nanoprobe sensors developed based on these substrates were able to detect the *Brucella* with LOD as low as 1.5×10^2 and 1.5×10^3 CFU/mL using K-r dipeptide and R-r dipeptide substrates, respectively, as the recognition element. The samples were tested using this sensor in few minutes. Cross-reactivity studies confirmed that the other proteases extracted from closely related pathogens have no significant effect on the sensor. To the best of our knowledge, this assay is the first assay that can be used with low-cost, rapid, direct, and visual detection of *B. melitensis*.



1. INTRODUCTION

Infectious diseases including those of viral origin are the main cause of the marked increase in human pathogenesis and death throughout the world exceeding even cancer and cardiovascular sicknesses.¹ Remarkable technological progress in sanitation has been made worldwide to identify, monitor, and control most infectious diseases.¹ Four different species of *Brucella* bacteria have been identified so far: *Brucella melitensis* (*B. melitensis*) (sheep, camels, and goats), *Brucella abortus* (cows, camels, elk, and buffalo), *Brucella suis* (pigs), and *Brucella canis* (dogs).² Bacteria of the genus *Brucella* can cause brucellosis. This disease is a highly contagious zoonosis and continues to have an impact significantly on livestock productivity, human health, and the well-being of local and national economies.³ Brucellosis is transmitted to humans through direct contact with infected animals or through the consumption of contaminated dairy products, especially cheese or raw milk. The *B. melitensis* bacterium is the most prevalent worldwide and the main cause of the most severe cases of brucellosis.⁴ The clinical picture of brucellosis often presents fever, sweating, arthralgia, hepatosplenomegaly, and lymphadenopathy.

Brucellosis has an annual worldwide occurrence rate of about 500,000 cases.^{5,6} It tends to spread more commonly in regions with poor animal healthcare programs and in areas where public health measures are not very effective.⁷ High-risk areas include the Middle East (Saudi Arabia and Yemen), the Mediterranean Basin (North Africa, Turkey, Spain, and Portugal), and Eastern Europe.³ Notably, the cases of Brucellosis in Saudi Arabia is increasing significantly.³

The human brucellosis disease lacks pathogenic symptoms, which make laboratory tests essential for its diagnosis. Brucellosis is usually diagnosed by isolating the organism from blood and body tissues, but this method is successful in only 40–70% of the cases.⁸

Received: January 6, 2024

Revised: March 6, 2024

Accepted: March 11, 2024

Published: May 6, 2024

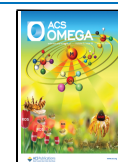




Figure 1. Screening of the FRET-based short peptide library for substrates prone to *Brucella* proteases.

One of the early observations in brucellosis is the finding that the sera of infected individuals contained agglutinating antibodies.⁹ A standard tube agglutination test (SAT) was developed to detect these antibodies and later adapted to the slide-agglutination format.¹⁰ However, this method was prone to false-negative results due to prozones, non-agglutinated IgG, and antibody blocking.⁹ Another serologic assay for brucellosis detection includes the Rose Bengal test (RBT), which is the most common screening test for brucellosis in both animals and humans. Interestingly, the RBT assay overcame SAT test issues.⁹ Nevertheless, the overall sensitivity reported for RBT varies widely due to variations in antigen sources and personal skills.^{11,12} Moreover, the RBT assay is time-consuming and lacks the ability to detect antibodies of all isotypes.¹³ Alternatively, enzyme-linked immunoassays were developed and evaluated to overcome these limitations with a satisfactory result.^{12,14}

Even though primary and binding conventional serological tests helped to eradicate brucellosis in many countries, these tests are not always sensitive or adequate to detect latent carriers of *Brucella*.¹⁵ Therefore, it was imperative to develop a test that is independent of circulating antibodies that may improve the diagnosis of brucellosis. A skin delayed-type hypersensitivity (SDTH) test was developed for this purpose.¹⁶

Over the past decade, there has been a major advancement in all aspects of molecular diagnostics with regard to human brucellosis.^{15,17} Polymerase chain reaction (PCR)-based tests have advantages over conventional methods as they are faster and more sensitive due to the non-infectious nature of DNA and therefore safer for laboratory personnel.¹⁸ PCR-based detection is also more reliable and specific when compared to the serum plate agglutination test (SPAT).¹⁹ However, for a PCR-based assay, a thermocycler is required which is difficult to be run in the field.

In this work, we present the development of a paper-based biosensor, designed to qualitatively and semiquantitatively detect *Brucella* extracellular proteases specifically. This assay is based on the use of a self-threaded peptide-based colorimetric probe. This probe constitutes a peptide recognition moiety conjugated to magnetic beads (mbs), which targets *Brucella* proteolytic activity as a biomarker. Colorimetric detection is realized through the dissociation of peptide substrate-mbs fixed

over a sensor gold band incorporated in the test strip. Compared to disease-related protease overexpression, this biosensor reflects the concentration of *Brucella* in the tested sample. This assay is rapid and cost-effective and applicable for the detection of clinical, food, and environmental samples. This *Brucella* protease biosensor represents a new detection approach that will lead to low-cost point-of-care devices for the sensitive detection and semiquantitation of *Brucella*. In addition, the described diagnostic device is portable and simple to operate by a nurse or non-skilled clinician making it appropriate for the low-resource setting.

2. EXPERIMENTAL SECTION

2.1. Materials and Reagents. Fluorogenic Bikkam substrates were synthesized by Pepmic Co., Ltd. (Suzhou, China) with a purity of >95%. The identity of the substrate was defined by mass spectrometry. The substrates' C-terminus was elongated with 1,6-aminohexanoic acid (Ahx) linked with a fluorescein isothiocyanate (FITC) probe, and at the N-terminus with a lysin-coupled DABCYL (KDbc) quencher. Carboxyl-terminated magnetic nanoparticles (50 nm in diameter) were provided by Turbobeats (Switzerland, sigma). *N*-Hydroxysuccinimide (NHS), 1-(3-(dimethylamino)propyl)-3-ethyl-carbodiimide (EDC), pH indicator stripes, potassium phosphate, sodium chloride, bovine serum albumin (BSA), ethylenediaminetetraacetic acid (EDTA), sodium azide, and Tris base were purchased from Sigma-Aldrich (Dorset, UK). A magnetic self-adhesive sheet was purchased from Polarity Magnets Company (Wickford, UK). Tryptone soy broth (TSB) and agar, brain heart infusion (BHI) broth, and trypticase soy broth (TS) were purchased from SDA, Oxoid, Ltd. (Basingstoke, UK). A sterile filter (0.22 μm) was obtained from Millipore (Watford, UK). The wash/storage buffer (10 mM tris, 0.15 M sodium chloride, 0.1% (w/v) bovine serum albumin, 1 mM ethylenediaminetetraacetic acid (EDTA), and 0.1% sodium azide, pH 7.5) and the coupling buffer (10 mM potassium phosphate and 0.15 M sodium chloride, pH 5.5) were prepared from chemicals of analytical grade.

2.2. Design and Synthesis of the FRET-Based Peptide Substrate Library. Peptide substrates selective to at least one of the *Brucella* extracellular proteases were screened by using a FRET-based di/tri-peptide library. Each peptide substrate was

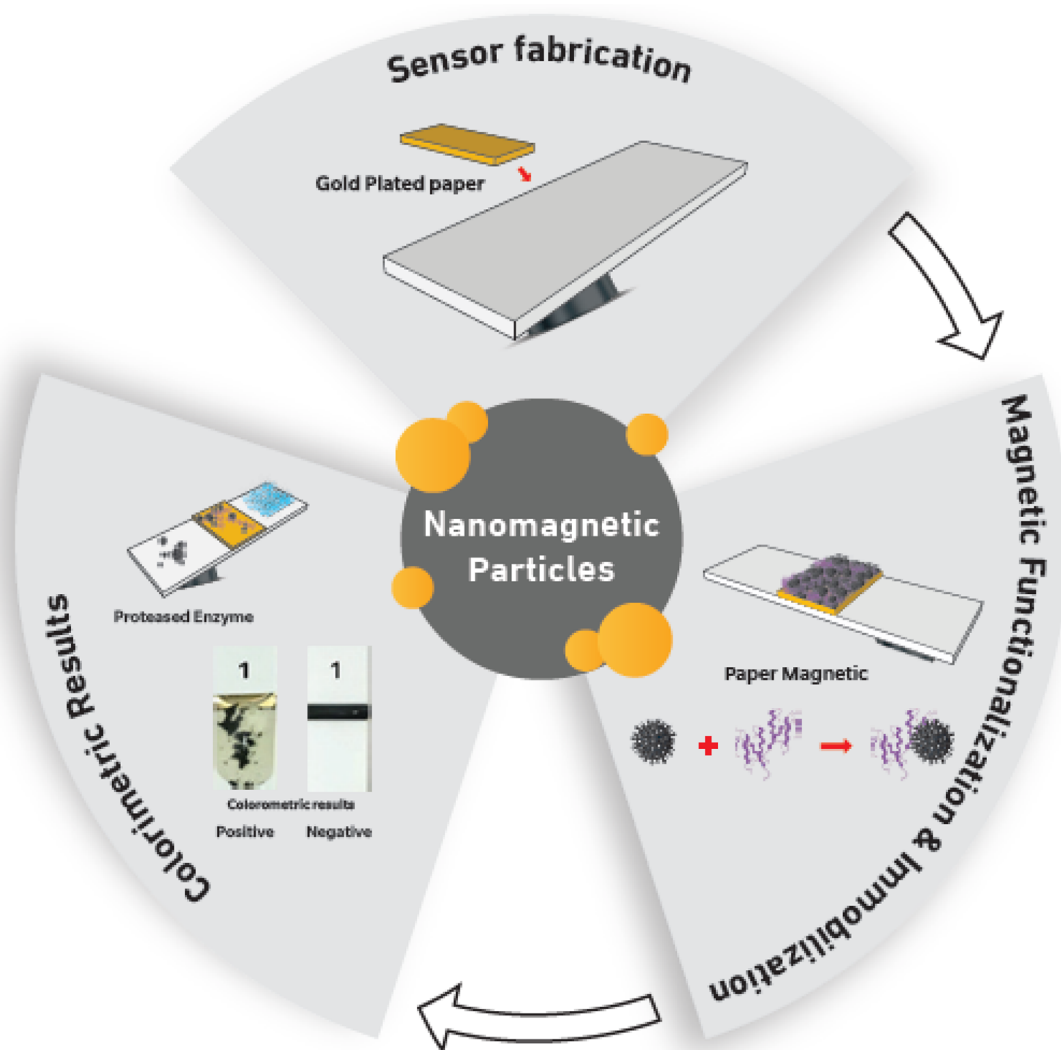


Figure 2. Principle of peptide-mbs nanoprobe functions step by step.

made up of L-amino acids, or C-terminal L-amino acid and N-terminal D-amino acid, or two D-amino acids. The upper-case letters represent L-amino acids, and the lower-case letter represents D-amino acids. Additionally, peptide substrate terminals were connected via a linker (6-aminohexanoic acid, Ahx) to a fluorescence donor and an acceptor group. As shown in Figure 1, all peptide substrates were labeled with fluorescein isothiocyanate (FITC) at the N-terminal and lysine followed by 4-(dimethylaminoazo)benzene-4-carboxylic acid (DABCYL) at the C-terminal. When FITC is excited, DABCYL absorbs photons from FITC emission and quenches the fluorescence effectively. However, in the presence of *Brucella* proteases, the specific short peptide substrates will be cleaved, and the FITC fluorophore and the DABCYL quencher are away from each other (Figure 1). Therefore, no fluorescence quenching will take place, resulting in bright fluorescence emission. The peptide library was constructed to contain a set of positively and negatively charged hydrophilic, aromatic, aliphatic natural (L), and unnatural (D) amino acids. The library contains 21 L-amino acid substrates, 20 D-amino acid substrates, and 74 L- and D-amino acid substrates. The Ahx spacer was applied between the FITC group and the peptide substrate for flexibility and to reduce the steric hindrance. Each

short peptide substrate was dissolved in dimethyl sulfoxide (DMSO), and the concentration was adjusted to 800 μM . The stock solutions were stored in the dark at $-20\text{ }^{\circ}\text{C}$ until further use.

2.3. Preparation of *B. melitensis* Culture and Extracellular Protease. The bacteria strain used in this study was kindly provided by the National Guard Hospital in Riyadh, and the experiment was performed in the third category lab. *B. melitensis* was grown on blood agar at $37\text{ }^{\circ}\text{C}$ for 48 h; from that, a single colony was isolated and cultured in TSB and incubated at $37\text{ }^{\circ}\text{C}$. After 18 h of growth, the bacterial cells were estimated by McFarland standards. The cell count was estimated to be 1.8×10^9 CFU/mL.

The *Brucella melitensis* total extracellular protease solution was obtained by centrifuging the bacterial culture at 3000g for 10 min. The culture supernatant was filtered using a $0.22\text{ }\mu\text{m}$ syringe filter. The filtrate proteolytic activity was directly proportional to the bacterial concentration (CFU/mL). Serial dilution was prepared to estimate the limit of detection of the sensor. Other infectious pathogens including *Escherichia coli* (*E. coli*) O:157 and *Yersinia enterocolitica* ATCC 55075 cultured in BHI broth and *Vibrio cholerae* ATCC 39315

cultured in TS broth were used as controls to tract the short peptide substrates selectively.

2.4. Fluorescence Resonance Energy Transfer Assay for Screening the *Brucella* Active Substrate. The specific peptide substrates against the proteolytic activity of *B. melitensis* from the total extracellular proteases were screened using a FRET-based high-throughput screening assay in a 96-well microtiter plate. We used 96 short peptide substrates having a FRET pair, labeled with the FITC fluorophore at the N-terminal and the DABCYL quencher at the C-terminal. The presence of *B. melitensis* extracellular proteases was monitored, and the *Brucella* protease activity (ability to cleave the peptide) was calculated based on the change in fluorescence measured. In this experiment, 0.5 μL of each peptide substrate from 800 μM solution was added to the microtiter plate wells containing 50 μL of PBS buffer. Subsequently, 50 μL of *B. melitensis* extracellular protease solution was added, and the change in the fluorescence intensity was monitored every 2 min for 2 h at 37 $^{\circ}\text{C}$ using a microtiter plate reader. The samples were excited in the wavelength range of 485 ± 10 , and emission was observed at a wavelength of 535 nm. The negative control (no protease) including a mixture of 50 μM PBS and 50 μL of TSB was used. The relative fluorescence unit increment for each substrate was calculated by subtracting the value of the negative control from that of the test substrate. The test was performed in triplicate under the same condition.^{20–22}

2.5. Isolation and Purification of *Brucella* DNA. Cultured *Brucella* was centrifuged at 8000g for 10 min to concentrate the bacterial cells into pellets. The supernatant was then discarded, and the pellet was suspended in a bacterial lysis buffer. The test volume was adjusted to 230 μL . Then, 100 μL of the concentrated bacteria suspension was transferred into the MagNA pure LC reagent/sample stage. DNA isolation and purification were performed automatically by the instrument. The isolated DNA was quantified using UV absorption of the DNA at 260 nm and stored at -20°C until further use.

2.6. Magnetic Beads (mbs) Functionalization. Carboxylic acid-functionalized mbs (15 mg/mL, Turbobeads, Zurich, Switzerland) were washed using a coupling buffer (10 mM potassium phosphate and 0.15 M sodium chloride, pH 5.5) as shown in Figure 2. Peptide substrates (1 mg/mL) synthesized by Pepmic Co., Ltd. (Suzhou, China) were dissolved in DMSO and mixed with freshly prepared coupling agents EDC (0.57 mg/mL) and NHS (12 mg/mL) (Sigma-Aldrich, Dorset, UK). The peptide and the coupling agent solutions were mixed at 4 $^{\circ}\text{C}$ for 18 h using an end-over-end rotator. The uncoupled short peptides were removed by several washes with a washing buffer.^{21–24} The remaining unreacted active sites in the beads were quenched by treating the mbs with 1% BSA for an hour in the coupling buffer. After completion of the blocking step, beads were washed with a wash buffer 5 times and stored at 4 $^{\circ}\text{C}$ in a wash buffer containing 0.02% sodium azide.

2.7. Sensor Fabrication and Immobilization. Self-adhesive tape purchased from Whatman (London, UK) was gold-plated using a sputtering machine at the School of Engineering at King Abdullah University of Science and Technology (KAUST, Thuwal, Saudi Arabia). A rectangular gold sensing platform ($\sim 1.5\text{--}2 \times 3$ mm) was incised and fixed over a waterproof physical support (Figure 2). The sensor served as biofunctionalization and immobilization of the monolayer-conjugated nanomagnetic beads.

The sensor platform was mounted with 30 μL of mbs conjugated with the peptide substrates (nanoprobe). The

sensor platform was left at room temperature until dryness was achieved to promote the disulfide linkage between the gold surface and the peptide substrate thiol groups. After which, an external magnet ($12.5 \times 12.5 \times 5$ cm), with strengths of 3360 and 573 gauss, was passed over the nanoprobe to remove unbound functionalized mbs. The developed nanoprobe sensor then showed a black color (Figure 2). The color change from gold to black after immobilization of the mbs-short peptides provides a colorimetric sensor platform. To accelerate nanoprobe cleavage following proteolysis, a round magnetic paper was installed at the back of the sensor (Figure 2). This magnet collected the cleaved mbs-peptide fragments restoring the sensor's original golden color.

2.8. Quantitative Measurement. The developed biosensor was designed as a colorimetric testing tool for the detection of *B. melitensis* extracellular proteases, specifically by tracking sensor nanoprobe color changes and, in particular, the change of the black color of the sensor to a golden color. The increase in the sensor golden color intensity reflects the amount of mbs-peptide fragments cleaved, which is in proportion to the *B. melitensis* extracellular protease concentration. Different concentrations of *B. melitensis* extracellular proteases were prepared by serially diluted supernatant solutions obtained from cultured *B. melitensis*. A wide linear range from 10^1 to 10^8 CFU/mL using a McFarland standard was examined in order to find out the sensing nanoprobe's limit of detection (LOD).

2.9. Real-Time Polymerase Chain Reaction (RT-PCR). The *Brucella* DNA was extracted according to the following procedure. The concentration of the DNA template was quantified by UV-absorption spectroscopy. The absorption ratio of A_{260}/A_{280} confirmed the purity of the extracted DNA. The DNA template was subjected to 10-fold serial dilution with a lower concentration of 10^{-2} fg/mL and the highest concentration of 10^5 fg/mL used as templates for RT-PCR. According to the manufacturer's protocol, a 2 \times PCR mix, a target assay mix, and the *Brucella* DNA template solutions were mixed, and the mixture was subjected to RT-PCR amplification. The PCR thermocycles were as follows: initial denaturation at 95 $^{\circ}\text{C}$ for 30 s and then 45 cycles of 95 $^{\circ}\text{C}$ for 30 s and 60 $^{\circ}\text{C}$ for 30 s. The relative fluorescence unit of the probe was plotted against the number of cycles.

3. RESULTS AND DISCUSSION

B. melitensis infection presented a major challenge for both health and financial facilities. This infection is responsible for human brucellosis worldwide including Saudi Arabia and the rest of the Middle East, where brucellosis is considered an endemic disease among people and camels.²⁵ Especially in the nomadic area, where a specialized medical diagnosis instrument is not available with the non-typical clinical picture of human brucellosis. On the other hand, less than 10% of human cases of brucellosis may be clinically recognized and treated or reported. Meanwhile, most cases are not recognized due to misleading non-specific manifestations and increasing unusual presentations.²⁶ Although lab tests are the key assays for proper diagnosis of brucellosis, these tests may overlook and misdiagnose the illness, owing to the difficulty of the diagnostic technique and the lack of experienced trainers. Accordingly, there is a need for developing a rapid, reliable, specific, unautomated, and early detection system of *B. melitensis* in clinical samples for early diagnosis and proper treatment.^{5,27,28}

Brucella proteases play an important role in the acquisition of nutrients for the growth, proliferation, survival, and invasion of microbes to a hostile host environment through the degradation of the host tissues' pathogenicity.^{29–31} In this study, we rely on *Brucella* protease proteolytic activity on a self-threaded peptide substrate identified by the FRET assay for *B. melitensis* detection.^{20,32–34} The use of an enzyme-based diagnostic tool based on the proteolytic activity of a protease enzyme was previously described by Loesche and co-workers.³⁵ A *B. melitensis*-specific protease substrate was utilized in the development of the paper-based colorimetric assay. *B. melitensis* specifically cleaved N-terminal L-amino acids and C-terminal D-amino acids with positive side-chain short peptides. No cleavage was observed with substrates containing only D-amino acid peptides.

Tailored substrates with the highest specificity (K-r-K and R-r-K) were attached to hexanoic acid (Ahx) at both terminals. In the absence of Ahx, the protease may not access the peptide bond due to steric hindrance; however, introducing an Ahx long-chain molecule between the substrate and the magnetic nanoprobe would enhance protease accessibility to the peptide bond near the surface of the nanoprobe. A cysteine amino acid was linked to the C-terminus of the substrates. When the cysteine-containing substrate is in contact with the gold surface, it forms an irreversible gold–thiol covalent bond resulting in the formation of a self-assembled monolayer (SAM) of peptide-mbs over the gold sensor surface (Figure 2) and the N-terminal of the peptide was attached to the mbs.

The fabricated sensor was examined to detect the proteolytic activity of *B. melitensis* protease by incubating 10^7 CFU/mL over the functionalized gold sensor surface for few minutes (Figure 2). Upon proteolysis, the peptide segment-mbs fragment was released and collected by the round magnet on the back of the sensor stripe (Figure 2). The change in the color of the sensor from black to gold reflects the intensity of the proteolytic activity and the amount of particle dissociation of the peptide-mbs (Figure 2).

3.1. Identification of Active Peptide Sequences. High-throughput screening of 96 fluorogenic short peptide substrates revealed two specific substrates against *B. melitensis* proteases. Short peptides such as dipeptides and tripeptides used in the screening process were labeled with FITC and DABCYL. In the absence of *B. melitensis* proteases, the fluorescence of the FRET substrate is very minimal as the fluorescence energy transfer from the fluorophore (FITC) to the quencher (DABCYL) is in close proximity to each other. The FRET phenomenon is highly dependent on the distance between the fluorophore and the quencher. Even a very minute variation in the distance would lead to a large fluorescence signal change. Under suitable physiological conditions, *Brucella* proteases would cleave the specific peptidic bond of the short peptide substrates. Accordingly, the FITC and DABCYL labels will physically separate away, and a significant increase in the fluorescence signal will be observed. The most specific substrates have the maximum fluorescence signal. Two peptide substrates (K-r and R-r) showed a high fluorescence change in the presence of *Brucella* protease compared to the rest of the peptide substrates (Figure 3). The increase in the fluorescence of each substrate was monitored and compared with other substrates, as shown in Figure 4. From the fluorescence signals, it is clear that the K-r dipeptide substrate is the highly selective substrate to *Brucella* proteases when compared to all other substrates in the library. Other substrates, K-h, K-k, K-K, F-R,

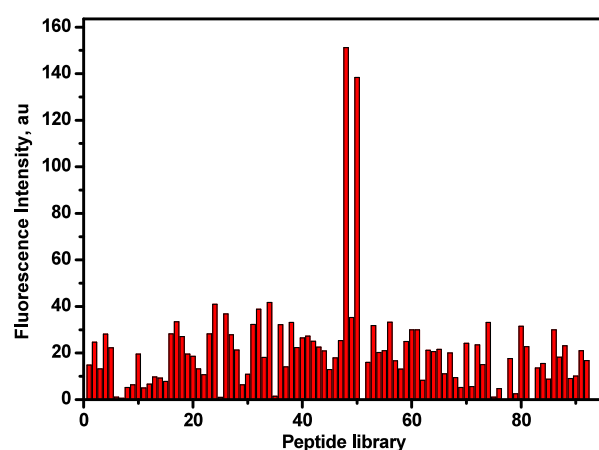


Figure 3. High-throughput screening of FRET peptide substrates specific for *Brucella melitensis* proteolytic protease. Among the library of fluorogenic substrates, K-r and R-r show high fluorescence intensity digested by the *Brucella* strains specifically cleaved N-terminal L-amino acids and C-terminal D-amino acid with positive side-chain short peptides. No significant change in the fluorescence intensity of substrates having only L-L or D-D amino acid-containing substrates.

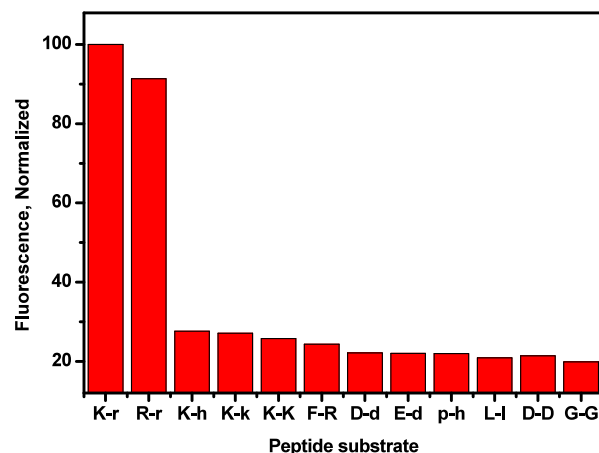


Figure 4. Change in the fluorescence intensities of the different fluorogenic peptides after 30 min of incubation with the strain culture. The *Brucella* strains specifically cleaved N-terminal L-amino acids and C-terminal D-amino acid with positive side-chain short peptides. No cleavage was observed only with D-amino acid-containing substrates.

D-d, and E-d, show a more than 20% increase in the fluorescence signal with respect to the K-r substrate presumably due to the insufficient *Brucella* protease activity on these dipeptide bonds. Notably, most of the susceptible substrates have L-amino acids in the N-terminal and D-amino acid in the C-terminal. More interestingly, all the active substrates have positively charged side chains like arginine (R) and lysine (K) at the C-terminals. This indicates that the *Brucella* protease specifically digests the substrate containing an L-amino acid with a positively charged side chain at the N-terminus. However, substrates having L-amino acids in the N-terminus and D-amino acid in the C-terminus with a negative charge such as isoleucine, glycine, and aspartic acid are highly resistant to *Brucella* proteases (Figure 4). From the fluorescence results, it is revealed that *Brucella* proteases can specifically cleave dipeptide substrates having L-amino acids at the N-terminus and D-amino acids at the C-terminus with

positively charged side chains, and they are not active on the negatively charged side chain as shown in Figure 4.

3.2. Real-Time PCR. Real-time PCR was carried out to confirm the presence of *Brucella*. The *Brucella* samples were cultured, and the DNA was extracted and used as a template for RT-PCR. The relative fluorescence increased exponentially with the increasing concentrations of the template as shown in Figure 5A. The fluorescence intensity of the sample containing

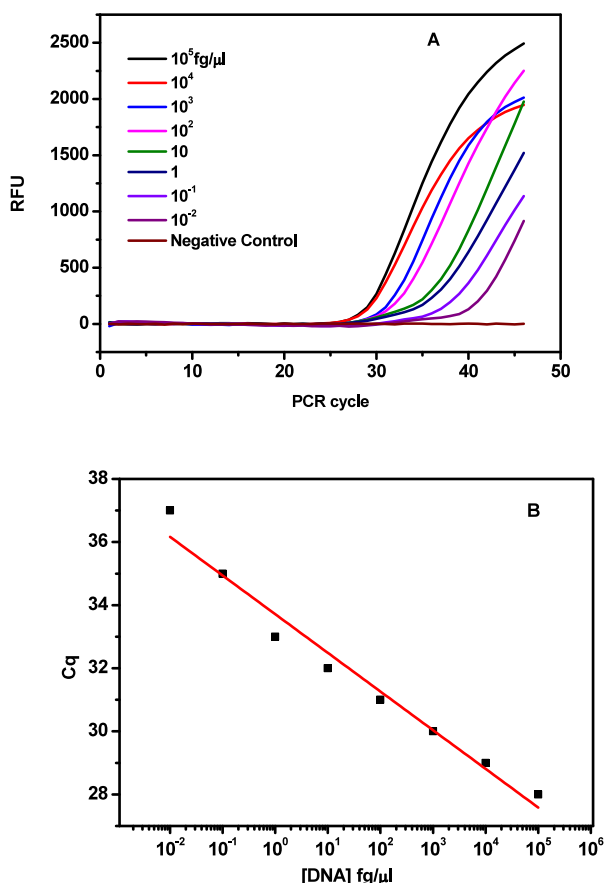


Figure 5. Real-time PCR carried out for *Brucella* species confirmation using the different concentrations of the template. (A) Increase in the relative fluorescence unit with the *Brucella* DNA template. (B) Increase in the relative fluorescence unit with the template diluted to 10^5 , 10^4 , 10^3 , 10^2 , 10, 1, 10^{-1} , and 10^{-2} fg/ μ L.

a high concentration (10^5 fg/mL) of the DNA template reached the threshold value of the fluorescence at cycle 27; however, the sample having the lowest concentration (10^{-2} fg/mL) reached the threshold value of fluorescence after 37 thermocycles. The results indicate that the RT-PCR was able to detect *Brucella* having very few copies of DNA. As shown in Figure 5B, the plot of C_q versus logarithmic *Brucella* DNA template concentration in the dynamic range of 0.01 to 10^5 fg/mL is linear. From the plot, it is clear that the limit of detection of this method is less than 0.01 fg/mL (Figure 5B), which is much less compared to our paper-based method. However, the paper-based method is a direct method without any amplification involved in the detection part, which can be used at the point of care and instrumentation-free. Results confirmed the presence of *Brucella* species in the sample, which further supports the results obtained from our newly fabricated sensor.

3.3. Quantitative Measurement. To detect the lowest limit of detection (LOD), two *Brucella* peptide-mbs nanoprobes utilizing K-r and R-r peptide substrates as a recognition moiety were subjected to nine different *B. melitensis* concentrations (1.5×10^8 , 1.5×10^7 , 1.5×10^6 , 1.5×10^5 , 1.5×10^4 , 1.5×10^3 , 1.5×10^2 , 1.5×10^1 , and 1.5×10^0 CFU/mL). Sensors were able to detect *B. melitensis* proteolytic activity with a LOD of 1.5×10^2 CFU/mL with the NH_2 -Ahx-K-r-Ahx Cys peptide sequence and a LOD of 1.5×10^3 CFU/mL with the NH_2 -Ahx-R-r-Ahx Cys sensor in 1 min (Figure 6). Visual reading of the LOD was validated side-by-side with that of the control.

Visual detection of the *B. melitensis* nanoprobe sensor 1 (K-r) and 2 (R-r) golden color as a result of *B. melitensis* protease proteolytic activity was simply viewed by the naked eyes (Figure 6). An increase in the sensor's golden surface is directly related to the increase in the concentration of *B. melitensis* culture (1.5×10^1 , 1.5×10^2 , 1.5×10^3 , 1.5×10^4 , 1.5×10^5 , 1.5×10^6 , 1.5×10^7 , and 1.5×10^8 CFU/mL) as shown in Figure 6A,B. The color change was quantified using ImageJ software (a public-domain, Java-based image processing program developed at the National Institutes of Health).³⁶ Peptide-mbs nanoprobe sensor images were captured by direct photography before and following *B. melitensis* protease application (Figure 6A,B). Sensor photos were processed through the red channel, which shows lower background levels. The color intensity of the black peptide-mbs layer was highlighted by the color threshold function with a red color, and then, the area of the total peptide-mbs was measured (Figure 6C-I,II). As the threshold adjustment process is subjective, the analysis was performed by two researchers who followed the proposed protocol. Next, the area of the cleaved peptide-mbs attracted by the backward magnet was measured (Figure 6D-I,II). The percentage of peptide-mbs cleaved was calculated by subtracting the area of the cleaved peptide-mbs from the total area. Calibration plots of the different *B. melitensis* concentrations indicate the linear correlation between percentage cleavages of peptide-mbs versus *B. melitensis* protease concentration. The linear part was fitted to linear regressions $y = -17.787x + 114.96$ ($R^2 = 0.9722$) and $y = -12.704x + 82.997$ ($R^2 = 0.9034$) in the concentration ranges of 10^3 – 10^8 and 10^2 – 10^8 CFU/mL for sensor 1 and sensor 2, respectively.

The *B. melitensis* peptide-mbs nanoprobe developed is sensitive and rapid in comparison to other reported label-free impedance biosensor, which detected *B. melitensis* in pure culture and milk samples with LOD values of 1×10^4 and 4×10^5 CFU/mL, respectively, in less than 1.5 h.³⁷ Another method using DNA-activated gold nanoparticles showed sensitivities down to 1000 CFU/mL for the detection of *Brucella* in 30 min.³⁸ Another visual spectrophotometric method using the genome DNA IS711 gene region was able to detect up to $1.09 \text{ pg } \mu\text{L}^{-1}$ unamplified *Brucella* genomic DNA.³⁹ Compared with the previously reported methods, our method is superior and has very low-cost production, and most importantly, one can test the presence of *Brucella* semi-quantitatively within a minute.

3.4. Cross-Reactivity Test. The *B. melitensis* sensor performance was validated by testing pure milk samples to ensure no cross-reactivity with the milk matrix. Results showed that the pure milk does not affect the sensor. For specificity purposes, the *B. melitensis* sensor was tested against the most common bacteria that are well-known to cause a cross-

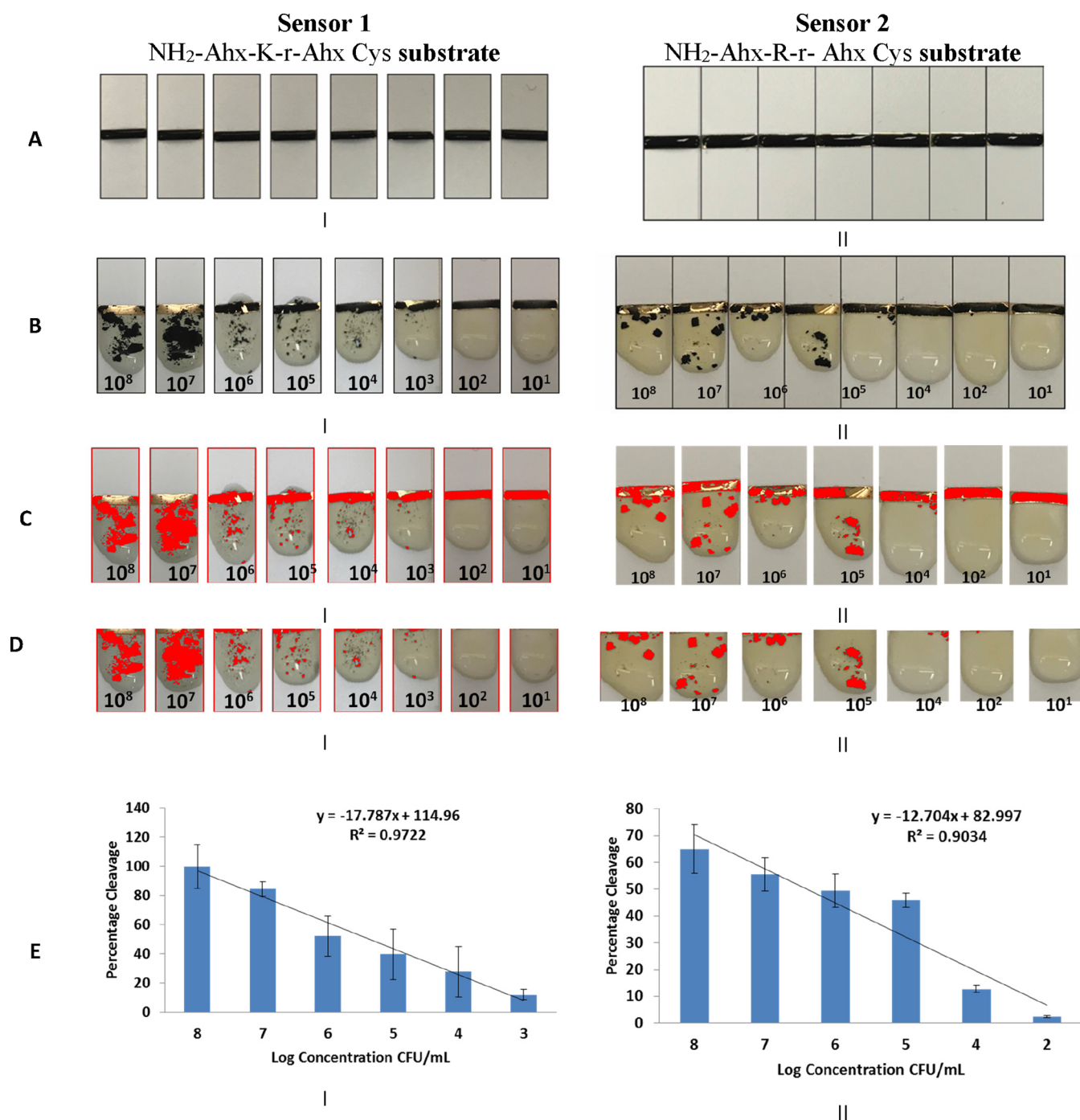


Figure 6. *Brucella melitensis* peptide-mbs nanoprobe using the Ahx-K-r-K-Ahx substrate (sensor 1) and Ahx-R-r-K-Ahx substrate (sensor 2) as a recognition moiety. (A) Ready-to-use *B. melitensis* peptide nanprobe for the detection *B. melitensis* proteases. (B) *B. melitensis* peptide nanprobe under the effect of different *B. melitensis* protease concentrations. The LOD is 10^3 and 10^2 CFU/mL for sensors 1 and 2, respectively. (C) JPG photo of the *B. melitensis* peptide nanprobe captured. Color intensity of the black peptide-mbs area on the sensor surface as processed by ImageJ software. (D) Cleaved peptide-mbs fragment attracted by the backward magnet as processed by ImageJ software. (E) Calibration plot of the different *B. melitensis* concentrations indicating the linear correlation between percentage cleavages of peptide-mbs versus *B. melitensis* protease concentration. The linear part was fitted to linear regressions $y = -17.787x + 114.96$ ($R^2 = 0.9722$) and $y = -12.704x + 82.997$ ($R^2 = 0.9034$) in the concentration ranges of 10^3 – 10^8 and 10^2 – 10^8 CFU/mL for sensor 1 and sensor 2, respectively.

reactivity with *B. melitensis*, especially with the serological tests, due to the similarity of the O-antigen side chain of LPS of *Brucella* as in *E. coli* O:157, *Yersinia enterocolitica* O:9, and *Vibrio cholerae*. As shown in Figure 7, the other proteases from the closely related bacteria did not influence the sensor probe, indicating the high specificity of the designed probe toward *B. melitensis*.

4. CONCLUSIONS

In this study, rapid, simple, easy-to-use, visual, and instrumentation-free assay was developed. This point-of-care detection has a signal that is visible by the naked eyes. The peptide-mbs probe sensor is based on the use of a self-threaded peptide substrate prone to cleavage selectively by *B. melitensis*



Figure 7. Specificity of the *Brucella* colorimetric peptide-mbs nanoprobe biosensor. (A) *Brucella* specific biosensor platform functionalized with black-colored peptide-mbs conjugates. (B) *Brucella* nanoprobe under the effect of *E. coli* O:157, *Yersinia enterocolitica* ATCC 55075, and *Vibrio cholerae*.

proteases and provide good sensitivity and selectivity. The *B. melitensis* detection sensor sensed *B. melitensis* proteases with an LOD of 1.5×10^2 CFU/mL with the Ahx-K-r-K-Ahx peptide sequence and an LOD of 1.5×10^3 CFU/mL with the Ahx-R-r-K-Ahx sensor in few minutes. No cross-reactivity with the milk matrix and with other well-known closely associated pathogens such as *E. coli* O:157, *Yersinia enterocolitica* O:9, and *Vibrio cholerae* has been observed. This colorimetric detection system can be applicable to detect other pathogens of interest.

AUTHOR INFORMATION

Corresponding Author

Mohammed M. Zourob – Department of Chemistry, Alfaisal University, Riyadh 11533, Saudi Arabia; orcid.org/0000-0003-2187-1430; Email: mzourob@alfaisal.edu

Authors

Sahar Alhogail – Department of Clinical Laboratory Science, King Saud University, Riyadh 11433, Kingdom of Saudi Arabia

Raja Chinnappan – Department of Chemistry, Alfaisal University, Riyadh 11533, Saudi Arabia

Ghadeer A.R.Y. Suaifan – Department of Pharmaceutical Sciences, Faculty of Pharmacy, The University of Jordan, Amman 11942, Jordan

Khalid M. Abu-Salah – Department of Nanomedicine, King Abdullah International Medical Research Center/King Saud bin Abdulaziz University for Health Sciences, King Abdulaziz Medical City, Riyadh 11481, Saudi Arabia

Khaled Al-Kattan – College of Medicine, Alfaisal University, Riyadh 11533, Saudi Arabia; Lung Health Centre, Organ Transplant Centre of Excellence, King Faisal Specialist Hospital and Research Centre, Riyadh 11211, Saudi Arabia

Dana Cialla-May – Institute of Physical Chemistry and Abbe Center of Photonics, Friedrich Schiller University Jena, Jena 07743, Germany; Center for Applied Research, InfectoGnostics Research Campus Jena, Jena 07743, Germany; Leibniz Institute of Photonic Technology, Jena 07745, Germany

Popp Jürgen – Institute of Physical Chemistry and Abbe Center of Photonics, Friedrich Schiller University Jena, Jena 07743, Germany; Center for Applied Research, InfectoGnostics Research Campus Jena, Jena 07743, Germany; Leibniz Institute of Photonic Technology, Jena 07745, Germany

Complete contact information is available at:

<https://pubs.acs.org/10.1021/acsomega.4c00192>

Notes

The authors declare no competing financial interest.

ACKNOWLEDGMENTS

M.M.Z. would like to acknowledge financial support from the research office at Alfaisal University.

REFERENCES

- (1) Martínez, J. L. Antibiotics and antibiotic resistance genes in natural environments. *Science* **2008**, *321* (5887), 365–367.
- (2) Scholz, H. C.; Hubalek, Z.; Sedlacek, I.; Vergnaud, G.; Tomaso, H.; Al Dahouk, S.; Melzer, F.; Kampfer, P.; Neubauer, H.; Cloeckert, A.; Maquart, M.; Zygmunt, M. S.; Whatmore, A. M.; Falsen, E.; Bahn, P.; Gollner, C.; Pfeffer, M.; Huber, B.; Busse, H. J.; Nockler, K. *Brucella microti* sp. nov., isolated from the common vole *Microtus arvalis*. *Int. J. Syst. Evol. Microbiol.* **2008**, *58* (2), 375–382.
- (3) Dean, A. S.; Crump, L.; Greter, H.; Schelling, E.; Zinsstag, J. Global burden of human brucellosis: a systematic review of disease frequency. *PLoS neglected tropical diseases* **2012**, *6* (10), No. e1865.
- (4) Vigeant, P.; Mendelson, J.; Miller, M. A. Human to human transmission of *Brucella melitensis*. *Canadian Journal of Infectious Diseases* **1995**, *6* (3), 153–155.
- (5) Aloufi, A. D.; Memish, Z. A.; Assiri, A. M.; McNabb, S. J. N. Trends of reported human cases of brucellosis, Kingdom of Saudi Arabia, 2004–2012. *Journal of Epidemiology and Global Health* **2016**, *6* (1), 11–18.
- (6) Elzein, F. E.; Sherbeeni, N. *Brucella* septic arthritis: case reports and review of the literature. *Case Rep. Infect. Dis.* **2016**, *2016*, 4687840.
- (7) Franc, K. A.; Krecek, R. C.; Häslér, B. N.; Arenas-Gamboa, A. M. Brucellosis remains a neglected disease in the developing world: a call for interdisciplinary action. *BMC Public Health* **2018**, *18* (1), 1–9.
- (8) Christopher, S.; Umopathy, B. L.; Ravikumar, K. L. Brucellosis: review on the recent trends in pathogenicity and laboratory diagnosis. *J. Lab. Physicians* **2010**, *2* (02), 055–060.
- (9) Díaz, R.; Casanova, A.; Ariza, J.; Moriyon, I. The Rose Bengal Test in human brucellosis: a neglected test for the diagnosis of a neglected disease. *PLOS Neglected tropical diseases* **2011**, *5* (4), No. e950.
- (10) Yildiz, F.; Tanyel, E.; Hatipoğlu, C. A.; Ertem, G. T.; Tülek, N.; Oral, B. Evaluation of *Brucella* tube agglutination test in patients with brucellosis, patients with bacterial infections other than brucellosis and healthy subjects. *Mikrobiyol. Bul.* **2005**, *39* (2), 211–217.
- (11) Blasco, J. M.; Garin-Bastuji, B.; Marin, C. M.; Gerbier, G.; Fanlo, J.; Jiménez de Bagués, M. P.; Cau, C. Efficacy of different Rose Bengal and complement fixation antigens for the diagnosis of *Brucella melitensis* infection in sheep and goats. *Veterinary record* **1994**, *134* (16), 415–420.
- (12) Cho, D.; Nam, H.; Kim, J.; Heo, E.; Cho, Y.; Hwang, I.; Kim, J.; Kim, J.; Jung, S.; More, S. Quantitative rose Bengal test for diagnosis of bovine brucellosis. *Journal of Immunoassay and Immunochemistry* **2010**, *31* (2), 120–130.
- (13) Kaltungo, B. Y.; Saidu, S. N. A.; Sackey, A. K. B.; Kazeem, H. M. A review on diagnostic techniques for brucellosis. *Afr. J. Biotechnol.* **2014**, *13* (1), 1.
- (14) Gall, D.; Nielsen, K.; Nicola, A.; Renteria, T. A proficiency testing method for detecting antibodies against *Brucella abortus* in

quantitative and qualitative serological tests. *Revue scientifique et technique* **2008**, *27* (3), 819.

(15) Yagupsky, P.; Morata, P.; Colmenero, J. D. Laboratory diagnosis of human brucellosis. *Clin. Microbiol. Rev.* **2019**, *33* (1), e00073-19.

(16) Bercovich, Z. The use of skin delayed-type hypersensitivity as an adjunct test to diagnose brucellosis in cattle: A review: (Summary of thesis, faculty of veterinary medicine, university of Utrecht, 1999). *Veterinary Quarterly* **2000**, *22* (3), 123–130.

(17) O'callaghan, D. Human brucellosis: recent advances and future challenges. *Infect. Dis. Poverty* **2020**, *9* (1), 1–2.

(18) Moeini-Zanjani, A.; Pournajaf, A.; Ferdosi-Shahandashti, E.; Gholami, M.; Masjedian, F.; Khafri, S.; Rajabnia, R. Comparison of loop-mediated isothermal amplification and conventional PCR tests for diagnosis of common *Brucella* species. *BMC Res. Notes* **2020**, *13* (1), 1–5.

(19) Khan, M. Z.; Zahoor, M. An overview of brucellosis in cattle and humans, and its serological and molecular diagnosis in control strategies. *Tropical medicine and infectious disease* **2018**, *3* (2), 65.

(20) Kaman, W. E.; Voskamp-Visser, I.; de Jongh, D. M. C.; Endtz, H. P.; van Belkum, A.; Hays, J. P.; Bikker, F. J. Evaluation of a D-amino-acid-containing fluorescence resonance energy transfer peptide library for profiling prokaryotic proteases. *Anal. Biochem.* **2013**, *441* (1), 38–43.

(21) Alhogail, S.; Suaifan, G. A. R. Y.; Bizzarro, S.; Kaman, W. E.; Bikker, F. J.; Weber, K.; Cialla-May, D.; Popp, J.; Zourob, M. On site visual detection of *Porphyromonas gingivalis* related periodontitis by using a magnetic-nanobead based assay for gingipains protease biomarkers. *Microchim. Acta* **2018**, *185* (2), 1–8.

(22) Alhogail, S.; Suaifan, G. A. R. Y.; Zourob, M. Rapid colorimetric sensing platform for the detection of *Listeria monocytogenes* foodborne pathogen. *Biosens. Bioelectron.* **2016**, *86*, 1061–1066.

(23) Levovich, A.; Lazarovitch, T.; Moran-Gilad, J.; Peretz, C.; Yakunin, E.; Valinsky, L.; Weinberger, M. Complex clinical and microbiological effects on Legionnaires' disease outcome; A retrospective cohort study. *BMC Infect. Dis.* **2016**, *16* (1), 75.

(24) Alhogail, S.; Suaifan, G. A. R. Y.; Zourob, M. Development of rapid and low-cost paper based sensing platform for bacterial detection. *Procedia technology* **2017**, *27*, 146–148.

(25) El-Koumi, M. A.; Afify, M.; Al-Zahrani, S. H. A prospective study of brucellosis in children: relative frequency of pancytopenia. *Mediterr. J. Hematol. Infect. Dis.* **2013**, *5* (1), e2013011.

(26) Mantur, B. G.; Amarnath, S. K.; Shinde, R. S. Review of clinical and laboratory features of human brucellosis. *Indian J. Med. Microbiol.* **2007**, *25* (3), 188–202.

(27) Faraz, A.; Kazmi, S. Y.; Farhan, M. A.; Ghaffar, U. B.; Hussain, S.; Irfan, A.; Salar, K. M. BRUCELLOSIS: BRUCELLOSIS AMONG CLINICALLY SUSPECTED PATIENTS ATTENDING A GENERAL HOSPITAL IN MAJMAAH SAUDI ARABIA. *Prof. Med. J.* **2018**, *25* (12), 1828–1832.

(28) Nabavi, M.; Hatami, H.; Jamaliarand, H. Epidemiological, risk factors, clinical, and laboratory features of brucellosis in the Southwest of Iran within 2009–2015. *Int. J. Prev. Med.* **2019**, *10*, 108.

(29) Horvat, R. T.; Parmely, M. J. *Pseudomonas aeruginosa* alkaline protease degrades human gamma interferon and inhibits its bioactivity. *Infection and immunity* **1988**, *56* (11), 2925–2932.

(30) Maeda, H. Role of microbial proteases in pathogenesis. *Microbiol. Immunol.* **1996**, *40* (10), 685–99.

(31) Barrett, A. J.; Woessner, J. F.; Rawlings, N. D. *Handbook of Proteolytic Enzymes*, Elsevier: 2012; Vol. 1.

(32) Contreras-Rodriguez, A.; Ramirez-Zavala, B.; Contreras, A.; Schurig, G. G.; Sriranganathan, N.; Lopez-Merino, A. Purification and characterization of an immunogenic aminopeptidase of *Brucella melitensis*. *Infection and immunity* **2003**, *71* (9), 5238–5244.

(33) Kaman, W. E.; Arkoubi-El Arkoubi, N. E.; Roffel, S.; Endtz, H. P.; van Belkum, A.; Bikker, F. J.; Hays, J. P.; Vadivelu, J. Evaluation of a FRET-peptide substrate to predict virulence in *pseudomonas aeruginosa*. *PLoS One* **2013**, *8* (11), e81428.

(34) Kaman, W. E.; Hulst, A. G.; van Alphen, P. T. W.; Roffel, S.; van der Schans, M. J.; Merkel, T.; van Belkum, A.; Bikker, F. J. Peptide-based fluorescence resonance energy transfer protease substrates for the detection and diagnosis of *Bacillus* species. *Analytical chemistry* **2011**, *83* (7), 2511–2517.

(35) Loesche, W. J.; Bretz, W. A.; Kerschensteiner, D.; Stoll, J.; Socransky, S. S.; Hujuel, P.; Lopatin, D. E. Development of a diagnostic test for anaerobic periodontal infections based on plaque hydrolysis of benzoyl-DL-arginine-naphthylamide. *Journal of clinical microbiology* **1990**, *28* (7), 1551–1559.

(36) Collins, T. J. ImageJ for microscopy. *Biotechniques* **2007**, *43* (1 Suppl), 25–30.

(37) Wu, H.; Zuo, Y.; Cui, C.; Yang, W.; Ma, H.; Wang, X. Rapid quantitative detection of *brucella melitensis* by a label-free impedance immunosensor based on a gold nanoparticle-modified screen-printed carbon electrode. *Sensors* **2013**, *13* (7), 8551–8563.

(38) Pal, D.; Boby, N.; Kumar, S.; Kaur, G.; Ali, S. A.; Reboud, J.; Shrivastava, S.; Gupta, P. K.; Cooper, J. M.; Chaudhuri, P. Visual detection of *Brucella* in bovine biological samples using DNA-activated gold nanoparticles. *PLoS One* **2017**, *12* (7), No. e0180919.

(39) Sattarahmady, N.; Tondro, G. H.; Gholchin, M.; Heli, H. Gold nanoparticles biosensor of *Brucella* spp. genomic DNA: Visual and spectrophotometric detections. *Biochemical engineering journal* **2015**, *97*, 1–7.